A&A 437, 929–933 (2005)
DOI: 10.1051/0004-6361:20052686
© ESO 2005

Astronomy & Astrophysics

Outflowing disk formation in B[e] supergiants due to rotation and bi-stability in radiation driven winds

M. Curé[1], D. F. Rial[2], and L. Cidale[3]

[1] Departamento de Física y Meteorología, Facultad de Ciencias, Universidad de Valparaíso, Valparaíso, Chile
e-mail: michel.cure@uv.cl
[2] Departamento de Matemáticas, Facultad de Ciencias Exactas y Naturales, Universidad de Buenos Aires, Argentina
e-mail: drial@dm.uba.ar
[3] Facultad de Ciencias Astronómicas y Geofísicas, Universidad Nacional de La Plata, La Plata, Buenos Aires, Argentina
e-mail: lydia@fcaglp.unlp.edu.ar

Received 11 November 2004 / Accepted 14 March 2005

Abstract. The effects of rapid rotation and bi-stability upon the density contrast between the equatorial and polar directions of a B[e] supergiant are re-investigated. Based on a new slow solution for different high rotational radiation-driven winds and the fact that bi-stability allows a change in the line-force parameters (α, k, and δ), the equatorial densities are about 10^2–10^4 times higher than the polar ones. These values are in qualitative agreement with the observations.

Key words. stars: early-type – stars: mass-loss – stars: rotation – stars: winds, outflows

1. Introduction

B[e] supergiants belong to a post-main sequence evolutionary stage of massive stars; their characteristics are: Balmer lines in emission, sometimes with P Cygni profiles with equivalent widths for H_α greater than 100 Å, low-excitation permitted emission lines; predominantly of singly ionized metals, forbidden emission lines of [O I] and [Fe II] and strong near/mid infrared excess due to hot circumstellar dust, indicating dust temperatures of 1000 K (Zickgraf et al. 1986, 1992).

A large percentage of B[e] supergiants (~70%−80%) show a hybrid spectrum (Zickgraf et al. 1985, 1986) that comes from the simultaneous observations of optical narrow low-excitation emission lines (~100 km s^{-1}) and broad UV high-excitation absorption lines (C IV, Si IV and N V) with terminal velocities similar to early B supergiant winds, of the order of ~1000 km s^{-1}. An empirical model that describes these hybrid spectral characteristics was suggested by Zickgraf et al. (1985) in terms of a two-component stellar wind, consisting of a fast radiation-driven wind (Castor et al. 1975, hereafter CAK) from polar latitudes and a slow and dense expanding disk in the equatorial regions of the star. This two-component wind has been confirmed from medium resolution spectropolarimetry for the evolved B[e] star HD 87643 (Oudmaijer et al. 1998).

The bi-stability mechanism induced by rotating radiation-driven winds was introduced by Lamers & Pauldrach (1991) to explain the formation of outflowing disks around early-type stars. This mechanism, which causes a drastic change in the wind structure, was thought to be related to the behaviour of the Lyman continuum optical depth, τ_L, with the stellar latitude. For $\tau_L < 1$ the wind is fast but for $\tau_L \gtrsim 3$ the wind is slow. The bi-stability manifests itself at certain spectral types or temperatures. Lamers et al. (1995) have determined terminal velocities, V_∞, of a large sample of early-type stars concluding that the bi-stability jump is present around $T_{\rm eff}$ = 21 000 K. Vink et al. (1999) have theoretically shown that the bi-stability mechanism is located at $T_{\rm eff}$ = 25 000 K and that it is mainly due to the radiative acceleration by iron, caused by the recombination of Fe IV to Fe III.

Pelupessy et al. (2000) have calculated the density contrast (the ratio between equatorial and polar densities) in a B[e] supergiant for rotationally-induced bi-stability models applying multi-scattering line-force parameters above and below the critical temperature of the bi-stability jump. They show that the ratio between equatorial and polar densities is about ~10, and state that this value is a factor 10 times smaller than Bjorkman's (1998) calculations. Porter (2003) also asserts the difficulties in modelling optical-near-IR emission for B[e] supergiants with a disk model density structure produced by either a bi-stability wind or a Keplerian viscous disk.

The Pelupessy et al. (2000) wind solutions were computed considering values of $\Omega = v_{\rm rot}/v_{\rm brkup} \lesssim 0.6$, where $v_{\rm rot}$ is the equatorial rotational speed and $v_{\rm brkup}$ is the break-up speed. However, B[e] supergiants are located near the Eddington limit (Zickgraf et al. 1986). Here, critical rotation speed is reached at a much lower stellar rotational speed. Velocities of about 200 km s^{-1} would make the star rotate sufficiently close to the break-up speed to produce observable effects. Consequently,

Article published by EDP Sciences and available at http://www.edpsciences.org/aa or http://dx.doi.org/10.1051/0004-6361:20052686
provided by CONICET Digital
brought to you by CORE
View

the wind characteristics near the equator are expected to differ from the polar wind. Langer (1998) proposes the Ω-mechanism for these type of stars. His model calculations suggest that despite the loss of angular momentum due to mass loss and increasing radius, a rapidly rotating massive main-sequence star could remain for a substantial fraction of its lifetime close to the so-called Ω-limit which designates the limit of critical (or break-up) rotation.

In order to investigate the influence of rotation in radiation-driven winds (even for a star rotating up to break-up rotational speed), Curé & Rial (2004) performed a topological analysis of the rotating CAK model, finding that the line-force parameter δ (Abbott 1982), that accounts for changes in the ionization of the wind, leads to a bifurcation in the solution topology as a function of the rotational speed, shifting the location of the critical point of the CAK (x-type) singular point downstream. Thus a higher mass-loss rate and lower terminal velocity wind is attained in comparison to the frozen-in ionization ($\delta = 0$) case.

Curé (2004) showed that the standard solution (hereafter the fast solution) of the m-CAK wind model (Friend & Abbott 1986; Pauldrach et al. 1986) vanishes for rotational speeds of ~0.7–0.8 $v_{\rm brkup}$, and there exists a new solution that is much denser and slower than the known standard m-CAK solution. We will call it hereafter the *slow* solution.

The purpose of this work is to re-investigate the formation of an equatorial disk-wind for rapidly rotating B[e] supergiants, taking into account: 1) the fast and slow solutions of rotating radiation-driven winds that depend on the assumed rotational speed and 2) bi-stability line-force parameters.

In Sect. 2 we discuss the adopted line-force parameters. In Sect. 3 we show results for CAK and m-CAK models with fast and slow solutions. Section 4 is devoted to the analysis of the influence of changes in ionization throughout the wind. Discussion and conclusions are presented in Sects. 5 and 6, respectively.

2. Rotating bi-stability parameters

In order to investigate the influence of the rotation and the bi-stability jump on forming a disk-wind, we solve the non-linear momentum equation for the CAK wind and for the m-CAK wind, in both polar and equatorial directions. Details and calculation methods used here for the CAK wind are found in Curé & Rial (2004) and for m-CAK in Curé (2004).

Prior to solving CAK and m-CAK momentum equations, we have to know the line-force parameters. The parametrization from Abbott (1982) of the line-force uses 3 parameters (α, k and δ). These parameters are obtained from the fitting of the net line acceleration of hundreds of thousands of NLTE line transitions computed by consistently solving the radiative transfer and hydrodynamics. A different approach to calculate the line-force parameters that include multi-line effects for temperatures above and below the bi-stability jump was developed by Vink et al. (1999). They use the Monte-Carlo technique and assume a β-field for the velocity law.

We want to stress, that no calculation of the line-force parameters has been performed for the slow solution and this is beyond the scope of this study. Therefore, in order to solve the wind momentum equation, we adopt the Pelupessy et al. (2000) line-force parameters, α and k, since they have been calculated for both sides of the bi-stability jump. These line-force parameters are summarized in Table 1.

Table 1. Bi-stability line force parameters.

T [K]	α	k	δ
30 000	0.65	0.06	0
17 500	0.45	0.57	0

3. Wind model results

In order to compare our results with the ones from Pelupessy et al. (2000), we adopt the same B[e] supergiant star they used: $T_{\rm eff} = 25\,000$ K, $M/M_\odot = 17.5$, $L/L_\odot = 10^5$ and solar abundance. For the lower boundary conditions for polar and equatorial directions, we use the same procedure as Stee & de Araujo (1994), i.e., after solving the momentum equation (CAK and m-CAK) in the polar direction, with the surface boundary condition, $\tau = 2/3$ (electron scattering optical depth), we obtain the value of the polar photospheric density, $\rho_{\rm p}(R_*)$. This value of the photospheric density is then used as surface boundary condition for the equatorial direction, for both CAK and m-CAK wind models, respectively.

In this work we have not taken into account either the change in the shape of the star or gravity darkening (von Zeipel effect) or the modification of the finite-disk correction factor due to the rotation (Cranmer & Owocki 1995, Eq. (26), Pelupessy et al. 2000). However, we expect that these effects may have a small influence on the fast solution (see Sect. 3.2.1). The study of their influences in the slow solution will be the subject of a forthcoming article.

3.1. The rotating bi-stable CAK wind

As a first step to study the combined effect of bi-stability and high rotation speed we investigate the CAK wind. We solve the isothermal ($T_{\rm eff} = 25\,000$) CAK wind for our B[e] supergiant; for the polar(equatorial) direction we use the line-force parameters determined for temperatures above(below) the bi-stability jump, see Table 1.

Figure 1 shows the density profile in both directions, polar (dotted line) and equatorial (continuous lines), for different values of the Ω parameter and Fig. 2 shows ratios between the equatorial, $\rho_{\rm e}$, and polar, $\rho_{\rm p}$, densities. Our result, without the finite-disk correction factor, gives a density contrast similar to the one obtained for $\Omega = 0.6$ by Pelupessy et al. (2000), who use the finite disk correction factor. The density contrast for $\Omega > 0.7$ are a few times denser. While the CAK model can be calculated for any rotational speed, Pelupessy et al. (2000) could not calculate m-CAK models for $\Omega > 0.6$, because the fast solution ceases to exist (Curé 2004). From Fig. 2, we can see that a disk wind structure is formed, the higher Ω, the denser and larger is the disk close to the photosphere and up to $r \sim 2R_*$, the region where the equatorial density reaches

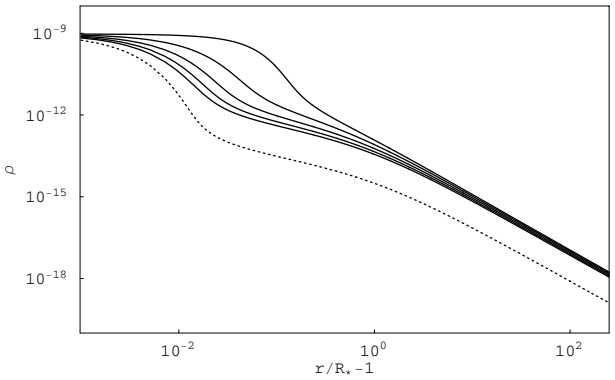

Fig. 1. CAK model: density (in g cm^{-3}) versus $r/R_* - 1$. Polar density is in dashed-line; equatorial densities are in continuous-line, the higher Ω, the higher the density (Ω = 0.6, 0.7, 0.8, 0.9, 0.99).

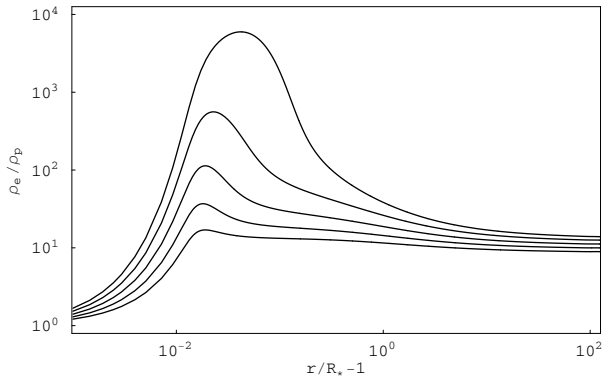

Fig. 2. CAK model: density ratio $\rho_e(\Omega)/\rho_p$ versus $r/R_* - 1$. The higher Ω, the higher the density contrast. Curves are for Ω = 0.6, 0.7, 0.8, 0.9, 0.99, respectively.

(as a function of Ω) values of hundreds of times the value of the polar density. Far from the stellar surface and up to hundreds of stellar radii, the ratio ρ_e/ρ_p reaches values of ∼10.

Hence, a rotating bi-stable radiation-driven wind forms a disk at the equatorial latitudes of these stars. Table 2 summarizes the polar and equatorial values of the terminal velocity, F_m, the "local mass loss rate" (see Pelupessy et al. 2000; Eqs. (10) and (11)) – the total mass loss rate if the solution for this latitude were valid for a spherical star – and the location of the critical (singular) point. The terminal velocities are higher than the observed ones in B[e] supergiant disks (Zickgraf 1998). This fact might be due to the assumed line-force parameters. There are no calculations of these parameters for the CAK model with rotational speeds. Therefore, these results represent our first approximation modeling of the outflowing disks of these objects.

3.2. The rotating bi-stable m-CAK wind

We present here the results of m-CAK wind models (see solution scheme in Curé 2004), taking the same set of line-force parameters given in Table 1 and different values of the rotational speed for the equatorial direction. Due to the fact that the existence of the fast or slow solution depends on the rotational speed, we analyse the fast solution for Ω = 0.6 (∼upper limit

Table 2. Parameters of the calculated CAK models: terminal velocity, V_∞ (km s^{-1}), F_m the local mass loss rate ($10^{-6}\,M_\odot\,yr^{-1}$) and r_c, the location of the critical point.

	Ω	V_∞	F_m	r_c/R_*
pole	0.0	826	0.181	1.60
equator	0.6	379	0.718	9.83
equator	0.7	348	0.730	11.47
equator	0.8	319	0.743	13.13
equator	0.9	293	0.756	14.80
equator	0.99	273	0.770	16.33

Table 3. Parameters of the calculated m-CAK models: terminal velocity, V_∞ (km s^{-1}), F_m, the local mass loss rate ($10^{-6}\,M_\odot\,yr^{-1}$) and r_c the location of the critical point.

	Ω	V_∞	F_m	r_c/R_*
pole	0.0	2287	0.109	1.027
equator[a]	0.6	747	0.724	1.057
equator	0.7	340	0.838	12.75
equator	0.8	312	0.851	14.21
equator	0.9	289	0.864	15.07
equator	0.99	266	0.875	17.14

[a] Fast solution values.

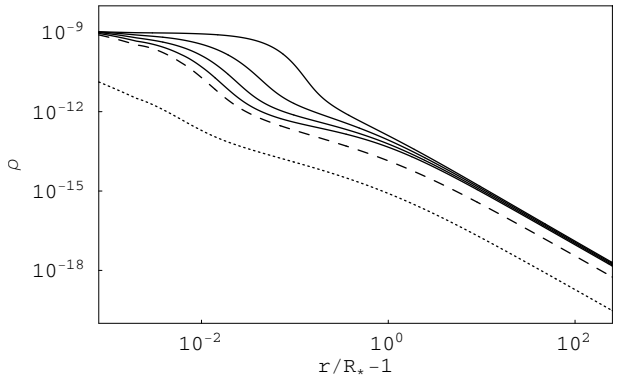

Fig. 3. m-CAK model: density (in g cm^{-3}) versus $r/R_* - 1$. Polar density is in dotted-line; equatorial density for Ω = 0.6 (fast solution) is in dashed-line and equatorial densities for Ω = 0.7, 0.8, 0.9, 0.99 are in continuous-line, the higher is Ω, the higher is the density.

of Ω for fast solutions) and then for higher rotational speeds we obtain slow solutions. We show that a disk-wind with a high density contrast is formed for high rotational speeds. Our results are summarized in Table 3, displayed in Figs. 3 and 4 and will be discussed below.

3.2.1. The fast solution

In order to compare our results with the ones from Pelupessy et al. (2000), we solve the m-CAK momentum equation, for Ω = 0.6. Note that there are no slow solutions that satisfy the lower boundary condition for this value of Ω.

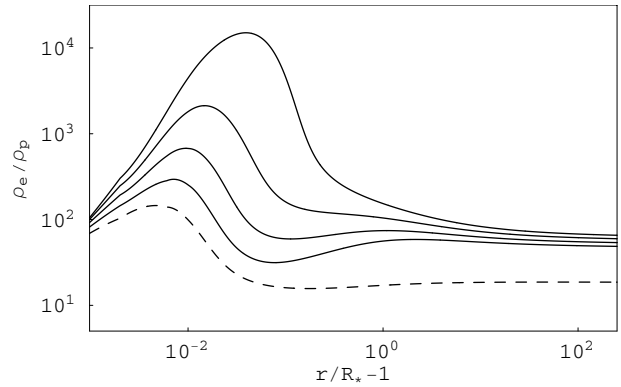

Fig. 4. m-CAK model: density contrast versus $r/R_* - 1$, dashed-line is for $\Omega = 0.6$ and continuous-line are for $\Omega = 0.7, 0.8, 0.9, 0.99$. The higher is Ω, the higher is the density contrast.

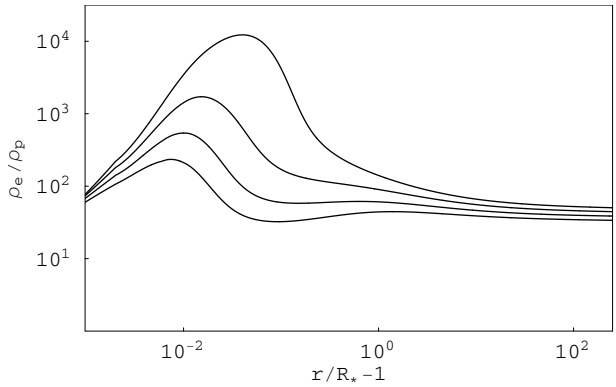

Fig. 5. Density contrast for the m-CAK wind with $\delta \neq 0$. Parameters α and k are given in Table 1.

The fast solution is shown in Figs. 3 and 4 by dashed-line. Its density is lower than the densities from slow solutions (continuous-lines, see Sect. 3.2.2) and higher than the polar density ($\Omega = 0$). We obtain a density contrast of about 10 for almost all the wind, similiar to the Pelupessy et al. (2000) result. Since Pelupessy et al. (2000) included the effects of changes in the shape of the star as a function of the rotational speed, dependence of the temperature on the latitude and the finite disk correction factor due to an oblate star, we expect that these effects have a small influence on the fast solutions.

The increase in the density contrast in the region close to the photosphere (see Fig. 4) is due to the centrifugal force and the consequently higher mass-loss rate of the fast solution when rotation is included (Friend & Abbott 1986).

3.2.2. The slow solution

We have calculated slow solutions from the m-CAK momentum equations in the equatorial direction for rotational speeds for $\Omega = 0.7, 0.8, 0.9, 0.99$. Density profiles from Figs. 1 and 3, for both CAK and m-CAK solutions respectively, show a similar behaviour. The differences near the photosphere and up to $\sim 2R_*$ are due to the finite disk correction factor, f_D, but for radii larger than two stellar radii, both density structures are almost the same. Near the photosphere f_D is less than one, thus a lower mass loss rate is attained. Further out in the wind the value of f_D is greater than one, so the plasma is accelerated to higher terminal velocities.

Figure 4 shows the density contrast profiles, which are larger than the corresponding CAK models (see Fig. 2). This is due to the inclusion of f_D in the momentum equation, giving a polar flow ($\Omega = 0$) less dense than the CAK case. Density contrasts reach values of around some thousands for radii less than $\sim 2R_*$ and a approximately a value of one hundred is maintained by the wind up to hundreds of stellar radii, almost independently of Ω. This result concerning the disk behaviour is in qualitative agreement with the values estimated from observations by Zickgraf et al. (1985, 1986, 1992), Zickgraf (1998), Oudmaijer et al. (1998) and Bjorkman (1998).

Table 4. Parameters of the calculated m-CAK models with $\delta \neq 0$ from Abbott (1982), terminal velocity, V_∞ (km s^{-1}), the local mass loss rate, F_m ($10^{-6}\ M_\odot\ \mathrm{yr}^{-1}$) and r_c/R_*, the location of the critical point.

	Ω	V_∞	F_m	r_c/R_*
pole	0.0	1475	0.097	1.053
equator	0.7	318	1.042	15.07
equator	0.8	292	1.087	16.04
equator	0.9	267	1.138	18.41
equator	0.99	248	1.188	19.88

4. Changes in ionization throughout the wind

Prinja et al. (2005) investigated the ionization structure of early-B supergiant winds and demonstrated that the wind ionization increases with distance from the star. This structure is different to the one exhibited by an O-star wind. Therefore in order to study the effect of changes in ionization with radial distance in a fast rotating supergiant, we explore the influence of the parameter δ in the m-CAK model.

We adopt δ values from Abbott (1982), for the polar direction, $\delta = 0.12$ ($T = 30\,000$) and for the equatorial direction, $\delta = 0.089$ ($T = 20\,000$). The α and k values are the ones from Table 1. Figure 5 shows density contrast profiles for $\Omega \geq 0.7$, which exhibit the same behaviour as in the frozen-in ionization case (Sect. 3.2.2) and values of the same order. We have also calculated m-CAK models with the δ line-force parameter from Shimada et al. (1994), arriving at the same conclusion that the δ-parameter has a small influence on the density contrast value. The model parameters are summarized in Table 4.

5. Discussion

We want to stress the importance of the combined effect of slow and fast solutions with bi-stable line-force parameters in forming an outflowing disk wind in B[e] supergiants. Density contrasts of the order of 10^2 up to large distances from the star are attained.

This theoretical value is in qualitative agreement with the values derived from observations of the order of 10^2–10^3 (Zickgraf et al. 1989; Zickgraf 1998, and references therein, Bjorkman 1998).

Previous simulations of disk formation in rotating radiation-driven winds induced by bi-stability have underestimated the density contrast, mainly due to: a) the use of a β-field (with $\beta = 1$, Lamers & Pauldrach 1991) to describe the wind velocity profile, even for high rotational speeds where this approximation fails (Curé 2004). Table 1 from Lamers & Pauldrach (1991) shows that $\tau_{\rm L} > 3$ exactly when the standard fast solution ceases to exist, and b) Pelupessy et al. (2000) calculations, based in the fast solutions, were restricted to values of $\Omega \leq 0.6$ and these rotation values are not high enough to develop a dense disk.

A dense disk is formed when the slow solution starts to exist. For our test star, this occurs for $\Omega \gtrsim 0.7$. This condition is in agreement with the estimation of $0.74 \leq \Omega \leq 0.79$ by Zickgraf (1998) in order to reproduce observable effects in the structure of stellar winds. However, observational rotation speeds of B[e] supergiants have high uncertainties, because only a few stars show photospheric absorption lines appropiate for the measurements of $V \sin(i)$. The inferred observational value of Ω lies in the range 0.4–0.7 (Zickgraf 1998).

We have verified that the δ line-force parameter, which is related to changes in ionization throughout the wind, modifies the wind structure, mass-loss rate, terminal velocity and location of the singular point (compare Tables 3 and 4). Despite these changes, the density ratio $\rho_{\rm e}/\rho_{\rm p}$ is almost the same as in the frozen-in ionization case.

Furthermore our results for the density contrast based on the m-CAK fast solution for $\Omega = 0.6$ are of the same order as Pelupessy et al. (2000), even though they included a more detailed description of the distortion of the star due to the rotational speed.

The existence of a fast solution for the polar direction and a slow solution for the equatorial direction, calculated using bistable line-force parameters, give a density contrast of the order of 100.

Since most of the B[e] supergiants in the H–R Diagram are located below the bi-stability jump temperature (25 000 K), in our conception, the theoretical explanation for the existence of a two-component wind model (Zickgraf et al. 1985) is due to the nature of the solutions of rapidly rotating radiation-driven wind. The change (jump) from the fast solution to the slow solution at some latitude yields to a two-component wind, where each solution structure has its own set of line-force parameters. This picture would be remarked for cases when the bi-stability jump is present.

Another important aspect to remark is the scarcity of self-consistent calculations of line-force parameters k, α, δ for the m-CAK fast solution and the lack of calculations for our slow solution. The uncertainty in the values of the parameters is reflected in the value of the terminal velocity, mass loss rate, as well as in the density contrast. Specifically, the predicted terminal velocities, see Tables 3 and 4, are about 2–3 times greater than values inferred by observations (Zickgraf 1998).

Therefore our results that combine fast and slow wind solutions are a first approximation to re-investigate disk formation in high rotating stars with radiation-driven winds. A detailed wind model needs a self-consistent line-force parameter calculations for both fast and slow solutions.

6. Conclusions

We have revisited radiative driven wind models for a rapidly rotating B[e] supergiant ($\Omega \gtrsim 0.6$) assuming a change in the line-force parameters due to the bi-stability jump. The existence of slow and fast solutions in the model predicts density contrasts which are of the order of 10^2–10^4 near the stellar surface ($r \lesssim 2\ R_*$), while outside they fall to values of about 10^1–10^2 and the disk extends up to ~100 stellar radii. Comparing the density contrast predicted by the CAK and m-CAK models, we conclude that the m-CAK model better describes disk formation in B[e] supergiants, being in qualitative agreement with observations.

Acknowledgements. This work has been possible thanks to the research cooperation agreement UBA/UV, UNLP/UV and DIUV project 15/2003.

References

Abbott, D. C. 1982, ApJ, 259, 282
Bjorkman, J. E. 1998, in B[e]stars, ed. A. M. Hubert, & C. Jascheck, ASSl 233 (Dordrecht: Kluwer), 189
Castor, J. I., Abbott, D. C., & Klein, R. 1975, ApJ, 195, 157
Cranmer, S. R., & Owocki, S. P. 1995, ApJ, 440, 308
Curé, M. 2004, ApJ, 614, 929
Curé, M., & Rial, D. F. 2004, A&A, 428, 545
Friend, D., & Abbott, D. C. 1986, ApJ, 311, 701
Lamers, H. J. G. L. M., & Pauldrach, A. W. A. 1991, A&A, 244, L5
Lamers, H. J. G. L. M., Snow, T. P., & Lindholm, D. M. 1995, ApJ, 455, 269
Langer, N. 1998, A&A, 329, 551
Oudmaijer, R. D., Proga, D., Drew, J. E., & de Winter, D. 1998, MNRAS, 300, 170
Pauldrach, A., Puls, J., & Kudritzki, R. P. 1986, A&A, 164, 86
Pelupessy, I., Lamers, H. J. G. L. M., & Vink, J. S. 2000, A&A, 359, 695
Porter, J. M. 2003, A&A, 398, 631
Prinja, R. K., Massa, D., & Searle, S. C. 2005, A&A, 430, L41
Shimada, M. R., Ito, M., Hirata, B., & Horaguchi, T. 1994, Pulsation; rotation; and mass loss in early-type stars (Dordrecht: Kluwer Academic Publishers), IAU Symp., 162, 487
Stee, Ph., & de Araujo, F. X. 1994, A&A, 292, 221
Vink, J. S., de Koter, A., & Lamers, H. J. G. L. M. 1999 A&A, 350, 181
Zickgraf, F.-J. 1998, in Habilitation Thesis, Univeristy of Heidelberg
Zickgraf, F.-J., Wolf, B., Stahl, O., Leitherer, C., & Klare, G. 1985, A&A, 143, 421
Zickgraf, F.-J., Wolf, B., Stahl, O., Leitherer, C., & Appenzeller, I. 1986, A&A, 163, 119
Zickgraf, F.-J., Wolf, B., Stahl, O., & Humphreys, R. M. 1989, A&A, 20, 206
Zickgraf, F.-J., Stahl, O., & Wolf, B. 1992, A&A, 260, 205